

Effect of blood activity on dosimetric calculations for radiopharmaceuticals

Alexandra Zvereva^{1,2}, Nina Petoussi-Henss¹, Wei Bo Li¹, Helmut Schlattl¹, Uwe Oeh¹, Maria Zankl¹, Frank Philipp Graner³, Christoph Hoeschen^{1,4}, Stephan G. Nekolla³, Katia Parodi², Markus Schwaiger³

¹Helmholtz Zentrum München, German Research Center for Environmental Health, Department of Radiation Sciences, Research Unit Medical Radiation Physics and Diagnostics, Ingolstädter Landstrasse 1, 85764 Neuherberg, Germany

²Ludwig Maximilians University (LMU) Munich, Experimental Physics – Medical Physics, Am Coulombwall 1, 85748 Garching, Germany

³Technische Universität München, Department of Nuclear Medicine, Ismaninger Str. 22, 81675 Munich, Germany

⁴Otto von Guericke Universität Magdeburg, Institut für Medizintechnik, Universitätsplatz 2, 39104 Magdeburg, Germany

Concise and informative title: Blood in internal dosimetry

Corresponding author:

Alexandra Zvereva

Ingolstädter Landstrasse 1, 85764 Neuherberg, Germany.

alexandra.zvereva@helmholtz-muenchen.de, Tel: +498931873247, Fax: +498931873846

Acknowledgements:

The work was done within the collaborative project PASSOS (<http://passos.helmholtz-muenchen.de>) funded by German Federal Ministry of Education and Research, grant 02NUK026.

We thank Matthias Greiter for fruitful discussions on compartmental pharmacokinetic modelling.

Abstract

Purpose The objective of this work was to investigate the influence of the definition of blood as a distinct source on organ doses, associated with the administration of a novel radiopharmaceutical for positron emission tomography-computed tomography (PET/CT) imaging – (S)-4-(3-¹⁸F-fluoropropyl)-L-glutamic acid (¹⁸F-FSPG).

Methods Personalised pharmacokinetic models were constructed based on clinical PET/CT images from five healthy volunteers and blood samples from four of them. Following an identifiability analysis of the developed compartmental models, person-specific model parameters were estimated using the commercial program SAAM II. Organ doses were calculated in accordance to the formalism promulgated by MIRD (Committee on Medical Internal Radiation Dose) and ICRP (International Commission on Radiological Protection) using specific absorbed fractions (SAF) for photons and electrons previously derived for the ICRP reference adult computational voxel phantoms. Organ doses for two concepts were compared: source organ activities in organs parenchyma with blood as a separate source (concept-1); aggregate activities in perfused source organs without blood as a distinct source (concept-2). Aggregate activities comprise the activities of organs parenchyma and the activity in the regional blood volumes (RBV).

Results Concept-1 resulted in notably higher absorbed doses for most organs, especially non-source organs with substantial blood contents, e.g. lungs (81% maximum difference). Consequently, effective doses increased in concept-1 compared to concept-2 by 5–9%.

Conclusions Not considering the blood as a distinct source region leads to an underestimation of the organ absorbed doses and effective doses. The pronounced influence of the blood even for a radiopharmaceutical with a rapid clearance from the blood, such as ¹⁸F-FSPG, suggests that blood should be introduced as a separate compartment in most compartmental pharmacokinetic models and blood should be considered as a distinct source in dosimetric calculations. Hence, blood samples should be included in all pharmacokinetic studies for new tracers if possible.

Keywords: PET; pharmacokinetic modelling; biodistribution; internal dosimetry; nuclear medicine

Introduction

PET is an extensively used diagnostic technique in nuclear medicine. Zanzonico [1] summarised a number of advantages and drawbacks of PET imaging. The drawbacks include that PET is a radiation-based modality. Thus it delivers radiation doses to patients and potentially increases risks of negative health effects. The knowledge of the kinetic distribution of radiopharmaceuticals and of the resulting organ doses from PET diagnosis offers opportunities for an optimisation of PET diagnostic procedures.

Pharmacokinetic (PK) modelling is a useful tool that mathematically describes and predicts the distribution of an injected material in the human body over time [2-5]. In the model, organs/tissues and functional entities are designated as separate compartments and the metabolism of the considered substance is described as transfer rates, usually defined as model parameters. Mathematically, compartmental pharmacokinetic (CPK) models are often described by a set of first-order linear ordinary differential equations. ICRP presented PK models for most currently used radiopharmaceuticals [4,5]; nonetheless, there is a need for PK models for novel radiopharmaceuticals.

The input data, required for setting up a CPK model, are time-resolved activities in the considered organs/tissues. ICRP [4] and Leggett et al. [6] recommend using the blood distribution model for the substances which remain largely in the blood to consider a fraction of the activity in the regions of interest (ROI), associated with the circulating blood. ROI activities are obtained from registered PET and CT images. For each organ/tissue the measured radiotracer activity represents the sum of the activity in the organ/tissue parenchyma and the activity in the blood content of this organ/tissue. The blood is distributed throughout the organs in vessels. The diameter of the vessels goes down to 4–9 micrometres for capillary [7] which is much smaller than the spatial resolution of both PET and CT. Hence the blood vessels cannot be discriminated. Therefore, the contributions of radiotracer activities in organs/tissues parenchyma and their blood contents to the total measured activity value cannot be distinguished.

If the investigated radiopharmaceutical is distributed mainly by blood, most of the model parameters are the transfer rates from blood to organs/tissues parenchyma and back. Hence, the values of the transfer rates, the definition of which is based on aggregate perfused organ activities, may be subject to large uncertainties, which might be propagated to the resulting

organ doses of the patients. Additionally, the way of considering blood activity in the dose calculation might considerably influence the resulting organ doses. This is true even for the relatively low activity concentrations in the blood because they can amount to high activities in the total blood volume (TBV) due to the large blood volumes (5300 ml and 3900 ml for reference male and female, respectively) [8].

Summarised in [4] PK models of some short-lived radionuclides were derived based on blood distribution model. Sgouros [9] corrected the activity of red bone marrow biopsy samples for blood contamination. Bigler and Sgouros [10] derived cumulated activities of oxygen in blood in various tissues according to the blood volume of each tissue. There is little done to discriminate the aggregate activities obtained from PET images from activities in blood and organ parenchyma in PK models, though, and the differences in organ doses due to the distinct consideration of blood source were not examined.

Our objective is to investigate the influence of defining of blood as a distinct source, i.e. RBV in various organs and blood vessels, in the dosimetry of the novel radiopharmaceutical ^{18}F -FSPG [11], developed for the diagnosis of malignant diseases. For this aim, activities in organ parenchyma and blood are separately considered in the developed CPK models. Two concepts of organ-dose computation are applied: activities in source organ parenchyma only, with blood as a separate source and aggregate activities in perfused source organs, without blood as a source. The comparison of the two aforementioned concepts is intended to demonstrate the importance of treating blood as a distinct source region.

Materials and methods

PET Images, blood and urine data

To evaluate the aforementioned concepts, we investigated human data using the novel radiopharmaceutical ^{18}F -FSPG. The PET images, blood and urine activities of five healthy volunteers (two men, three women) were acquired at the Nuclear Medicine Department of Klinikum rechts der Isar of Technische Universität München as part of the characterisation of this agent by Smolarz et al. [11]. The ethics committee approval had been already granted for the study [11].

For convenience, the following nomenclature for naming the volunteers will be used here and in the consecutive text: 1101/94, 1102/94, 1103/94, 1104/94, 1105/94.

Non-image information (age, height, weight of the volunteers) and the injected activities (IA) are presented in Table 1. Blood samples of volunteer 1102/94 were not taken. The used imaging protocol comprised seven sequential scans. The total body scan was obtained instantly after the tracer injection and the other six scans were done from the top of the head to the mid-thigh. Smolarz et al. [11] compensated the off-image activity in the partial body scans. The volunteers were followed up to 4.5 hours after the tracer administration. To resolve the high-gradient part of the time-activity curve, the frequency of the scans was higher at the beginning compared to later times. The measurement protocol is described in detail elsewhere [11].

The activity concentrations were determined for various ROI [11]. Using the organ volumes defined from the registered CT images, absolute activity values in the source organs were calculated.

Compartmental pharmacokinetic models and parameter estimation

To develop the CPK model structure, aggregate measured activities were used. To describe the kidney-urinary path we utilised elements of the commonly used ICRP urinary excretion model [12], which approximates the model reported in ICRP 53 and 128.

The CPK model structure that we proposed for the radiopharmaceutical ^{18}F -FSPG is presented in Figure 1. Model structural identifiability was tested against the measured data (PET images, blood samples) using the computer programme DAISY [13]. The considered ROIs included kidneys, bladder, heart, thyroid, salivary glands, pancreas, stomach wall, liver

and spleen [11]. These organs were initially implemented into the proposed model as compartments connected to the central blood compartment. We added sub-compartments for liver and spleen to better fit the measured data, analogously to, e.g., ICRP [12] and Giussani et al. [14], who introduced two liver sub-compartments. Sub-compartments 1 and 2 represent, respectively, short- and long-term retention of ^{18}F -FSPG. Liver-2 and spleen-2 are defined on a kinetic rather than a biological basis.

To describe the urinary excretion of ^{18}F -FSPG initially the kidney-bladder model reported by the ICRP [12] was adopted. It includes the direct transfer from blood to the urinary bladder and the slower transfer to the bladder through the urinary path. During the model fit, the transfer rate representing the direct flow from the blood to the bladder content could not resolve the relatively slow experimentally measured uptake of ^{18}F -FSPG by bladder. Therefore, we modified the ICRP urinary excretion model by removing the fast transfer from blood to bladder. To model the observed fast renal clearance and the slow uptake by bladder, an additional compartment was introduced between kidneys and bladder. Physiologically it represents the urine flow through the ureter (Supplemental Data, Figure 1).

Exact voiding times of the volunteers were recorded. This enables a volunteer-specific modelling of the urinary excretion. To account for the residual urine volume following void, promulgated in other published bladder models [15], an additional equation was included at every time-point of the voiding cycle Eq.(1):

$$q_{bladder} = q_{bladder} \times (1 - fr_i) \quad (1)$$

where $q_{bladder}$ denotes the activity in the bladder-content compartment and fr_i is the voiding fraction of void i with $0 \leq fr_i \leq 1$. We included fr_i as additional parameters into the CPK model.

The duration of the measurements covered 4.5 hours, and not the entire modelled time-period of 1000 minutes (≈ 16.7 hours). To account for the urinary excretion of activity after the last recorded voiding, we considered a scheme used by MIRD [15]: 3-hours voiding intervals following the last measured void and a 6-hours nighttime gap beginning at midnight. Due to the absence of experimental data later than 4.5 hours after the injection we assumed these later voids to be complete.

One compartment, defined as rest of body (RoB), was added to the model to account for the radiotracer activity transported to the organs/tissues that were not explicitly considered in the

CPK model. The RoB activities were calculated via the subtraction of measured organ activities from the total body data.

One common model structure was used for each volunteer; however, personalised model parameter sets were estimated based on the individual PET images and measured blood samples. A system of linear first-order ordinary differential equations was used to describe the kinetics of ^{18}F -FSPG. Model parameters were estimated using the commercial software SAAM II [16]. We performed the numerical fitting simultaneously for all transfer rates. All transfer rates were adjustable. Where $f r_i$ were indeterminable due to the absence of the experimental data, we fixed them to one (complete voiding). Reference values of TBV [8] were used.

Blood content of organs and tissues

Here we propose a method to separately consider activities in organ parenchyma and blood in the CPK models. A model fit was executed using aggregate activities of perfused organs as obtained from the PET images. To consider that aggregate activities comprise the activities of organs parenchyma and blood, each measured organ activity was associated with the respective organ compartment and a fraction of the blood compartment corresponding to its RBV. Reference RBV and TBV reported by ICRP [8] were used, because individual data for the studied volunteers are not available. The blood compartment was associated with the measured activities in blood samples.

Internal dosimetry

Organ absorbed dose coefficients were estimated according to the schema promulgated by MIRD [17]. The absorbed dose coefficient $d(r_T, T_D)$ in the target region r_T is calculated by

$$d(r_T, T_D) = \sum_{r_S} \tilde{a}(r_S, T_D) S(r_T \leftarrow r_S) + \tilde{a}(r_{RoB}, T_D) \left(\frac{M_{TB} S(r_T \leftarrow r_{TB}) - \sum_{r_S} M_{r_S} S(r_T \leftarrow r_S)}{M_{RoB}} \right) \quad (2)$$

with

$$S(r_T \leftarrow r_S) = \sum_i E_i Y_i \Phi(r_T \leftarrow r_S, E_i) \quad (3)$$

and

$$\Phi(r_T \leftarrow r_S, E_i) = \frac{\phi(r_T \leftarrow r_S, E_i)}{M_{r_T}} \quad (4)$$

where T_D is the dose-integration period (here 1000 minutes); $\tilde{a}(r_s, T_D)$ and $\tilde{a}(r_{RoB}, T_D)$ are the time-integrated activity coefficients (TIACs) in r_s (source region) and RoB; E_i, Y_i are mean energy and yield of radiation i ; $\phi(r_T \leftarrow r_s, E_i)$ and $\Phi(r_T \leftarrow r_s, E_i)$ are absorbed fraction and SAF, respectively; M_{r_T}, M_{r_s} and M_{RoB} denote the masses of target region, source region and RoB, respectively.

In this work two concepts were considered: the activities in source organ parenchyma were used, blood was a distinct source region (concept-1); the activities in perfused source organs, i.e. including activities in RBV, were used, blood was not a distinct source region (concept-2). In concept-2 blood activity was attributed to the source organs according to RBV, given by ICRP [8], the remaining blood activity was included into the RoB. In concept-1 M_{RoB} and M_{r_s} correspond to the respective masses without blood, in concept-2 to those with blood. We used SAF for photons and electrons, previously simulated with Monte Carlo methods [18] for the ICRP reference adult voxel phantoms [19].

SAF values used for the dosimetry in the current work have been originally simulated for organs with blood [18,19]. This corresponds to concept-2; nonetheless for concept-1 SAF corresponding to organ parenchyma are needed. For all combinations of source and target regions except source region RoB, the SAF for the organs containing blood (perfused organs) can be used as the SAF corresponding to the organs without blood (organs parenchyma). This can be understood if one considers the absorbed fraction ϕ . Note that index “w” refers to the case of perfused organs, “w/o” to organ parenchyma. The probability that a particle is absorbed in any constituent of an organ is proportional to its mass and its mass-energy absorption coefficient. This is valid for the self-irradiation and the cross-fire. Therefore:

$$\frac{\phi_{w/o}}{\phi_w} \approx \frac{M_{r_T w/o}}{M_{r_T w}} \quad (5)$$

In Eq.(5) the difference between the mass-energy absorption coefficients, $\frac{\mu_{en}}{\rho}$, between perfused organs and organ parenchyma is ignored because in the considered energy range this difference is small.

According to the definition of SAF and considering Eq.(5):

$$\Phi_{w/o} = \frac{\phi_{w/o}}{M_{r_{T w/o}}} \approx \frac{\phi_w}{M_{r_{T w/o}}} \cdot \frac{M_{r_{T w/o}}}{M_{r_{T w}}} = \frac{\phi_w}{M_{r_{T w}}} = \Phi_w \quad (6)$$

Thus, the SAF for all combinations of source and target regions except source region RoB, are approximately the same for both concepts – with and without blood.

To calculate the organ doses, an in-house software was used, which utilises pre-calculated SAFs for several gamma-ray energies and for detailed beta spectra from ICRP [20]. ^{18}F is a positron-emitter with mean energy of 249.8 keV. The pre-calculated SAFs for the corresponding electron energies and a photon energy of 511 keV (annihilation photons) were used. Note that the effective dose coefficients calculated here are not in accordance to the definition given by ICRP [21] because they are not age- and sex-averaged. They were computed for individual phantoms as weighted average of the individual organ equivalent dose conversion coefficients using tissue weighting factors from ICRP 103 [21]. This was done only for comparison purposes.

Results

Proposed CPK model structure

The developed model structure for ^{18}F -FSPG is presented in Figure 1. With the available experimental data the model structure was globally identifiable – as tested with the DAISY software.

Predictions of personalised CPK models

The subset of the resulting CPK model predictions along with the measured data is presented in Figure 2.

The retention of activity in the liver of volunteer 1102/94 was considerably higher compared to the other volunteers. The uptake in pancreas for volunteers 1102/94, 1104/94 and 1105/94 was similar, while for volunteer 1103/94 the maximum uptake in pancreas was approximately only half of that value, followed by a slower decline of activity in this organ. We observed different accumulation and release of activity in the stomach walls of the volunteers (see Figure 2).

^{18}F -FSPG showed relatively fast release from the body via the urinary excretion pathway. After the first void, 30–40% of the IA was excreted. However, such a renal clearance results in substantial doses from ^{18}F -FSPG for kidneys and urinary bladder wall.

Estimated model parameters and calculated TIACs for each volunteer are summarised in Supplemental Tables 2–6. We attributed the activity in the ureter compartment to the RoB compartment. The ureter was a part of the source RoB.

Organ dose coefficients and effective doses

Table 2 and Supplemental Table 7 show the resulting organ absorbed dose coefficients, effective-dose coefficients and the corresponding relative differences of concept-1 compared to concept-2.

For all source organs, except heart and spleen, no substantial differences between the two concepts were observed with the maximum difference of 6.7%, 5.2% and 3.7% for liver, thyroid and salivary glands, respectively. The doses for heart and spleen slightly increased in concept-1 compared to concept-2 (22.3% and 11.1% in maximum, respectively).

For most of the target organs, that are not sources, absorbed dose coefficients were considerably higher in concept-1 (up to 81%). Consequently, the effective dose coefficients in concept-1 were higher for all volunteers with a mean difference of 7.6% (median 8.3%). We observed considerable inter-individual variability in effective-dose conversion coefficients among the volunteers within each concept: 0.012–0.018 mSv/MBq (concept-1) and 0.011–0.016 mSv/MBq (concept-2).

Discussion

A method of modelling separately the blood contents of source organs was proposed, implemented and evaluated. According to it, the aggregate activities of perfused organs were directly used in the modelling as being associated with both the respective organ compartment and a fraction of the blood compartment. This method was successfully implemented into the developed CPK models for a novel radiopharmaceutical such as ^{18}F -FSPG. It allows a more precise modelling of the distribution of the radiopharmaceutical. It has some methodological limitations though. Reference values for TBV and RBVs were applied in personalised CPK models. The individual blood volumes in the various organs cannot be easily known and were not obtained by Smolarz et al. [11] as it was not within the scope of the study [11]. Leggett and Williams [22] showed considerable variability in the RBVs in various pools. Hence the utilisation of reference values here considerably contributes to the uncertainty of dose estimates.

The developed compartmental models satisfactorily describe the experimental data and show considerable inter-individual variability among the studied subjects, though some assumptions were made here as well. These assumptions mainly concern the scaling of partial body activity to the total body activity, done by Smolarz et al. [11]. Such scaling introduces additional uncertainties into the CPK modelling result because it eliminates possible inhomogeneity of activity distribution and uptake by different body tissues that are not present on the image. This uncertainty can be theoretically avoided by obtaining only whole body PET scans, but it requires longer measurement time and more discomfort for the patient. Hence we consider these assumptions to be appropriate and not critical for the CPK modelling result.

Comparison of our results for ^{18}F -FSPG with the study of Smolarz et al. [11] shows the importance of bladder-voiding intervals for the dose to bladder wall, as already demonstrated by other authors [14,15,23]. We considered individual voiding schemes whereas Smolarz et al. [11] assumed 3.5 h voiding intervals. For all volunteers, the first void took place at 0.86 ± 0.06 h after injection and the second void at 2.07 ± 0.29 h. Due to the fast renal clearance of ^{18}F -FSPG, voiding intervals of 3.5 h result in notably higher calculated doses to the bladder wall. Consequently, effective doses are overestimated in the study presented at [11].

SAFs for ICRP reference voxel phantoms [18,19] were used for dose computing. Hence, possible anatomical variability within the subjects was disregarded here and the computed doses are not individual-specific. Personalised dosimetry would require the usage of individual anthropomorphic phantoms. Nonetheless, to illustrate the differences between the two ways to treat the blood activity and its contribution to organ doses, applying the reference phantoms was sufficient.

The comparison of organ absorbed dose coefficients between concept-1 (activities in source organs parenchyma, RBV in various organs and blood vessels comprise the blood source) and concept-2 (activities in perfused source organs, without blood as a distinct source region) revealed notably higher doses in concept-1 for many organs. This was mostly observed for target organs with substantial blood fraction that are not sources, i.e. they are part of RoB, due to the higher contribution of blood activity to the self-absorption in concept-1. For organs that are part of RoB, the blood activity being attributed to the organs, according to RBVs (concept-1), leads to a higher dose than if the blood activity would be homogeneously distributed in all organs, comprising RoB (concept-2). This can be demonstrated on a specific example – the lungs (where the difference between the two considered concepts was the highest) of subject 1101/94 (Supplemental Table 8).

For most of the source organs no substantial differences between the two concepts were noticed. This was expected because, from one hand, the TIACs, and, therefore, the self-absorption, decreased in concept-1 due to the subtraction of RBV activities. From another hand, for the blood being present in all organs, a blood activity corresponding to the RBV was present in concept-1 in all source organs. Thus, the subtracted activities were effectively “placed back” to the source organs, compensating the self-absorption and leading to the same dose as for concept-2 (ignoring other cross-fire).

The observed differences in absorbed doses for heart wall and spleen are due to the cross-fire from the neighboring organs.

We assumed homogeneous distribution of blood in the organs. Thus the self-absorption effect of blood, being inside blood vessels, demonstrated by Hänscheid et al. [26], was not considered here, apart from the big blood vessels that are segmented in ICRP reference voxel phantoms [19]. A proper consideration of this effect in the entire body would require detailed information on the distribution of blood vessels [26].

The greatest impact of considering blood as a source region in dosimetry of ^{18}F -FSPG was observed for lungs, small intestine, colon, oesophagus, thymus, adrenals and extrathoracic airways – the organs that are important for the assessment of risks of radiation induced negative health effects. Due to high mass fractions of blood in liver, kidneys and spleen, great impact of blood activity in dosimetric calculations for these organs is expected in case of other radiopharmaceuticals, if the aforementioned organs are not sources. For radiopharmaceuticals with slower clearance from the blood than that of ^{18}F -FSPG, the effect of blood on dosimetric calculations is expected to be even more pronounced. The majority of the recent publications, related to dosimetric characterisation of new diagnostic and therapeutic agents [11,24,25], derive the dosimetry using OLINDA/EXM [27]. It does not utilise blood SAFs. Our results reveal that the absorbed doses for target organs with substantial blood fraction might be underestimated in this case.

Conclusion

To delineate realistic dosimetry we developed individual CPK models and investigated the effect of blood as a distinct source region on dosimetry. Considerable inter-individual variability in the pharmacokinetic behaviour was shown. It helps to understand the intrinsic uncertainties when reference models are applied to individuals and justifies the benefit of personalised modelling approaches. We demonstrated a high influence of blood activity on the organ absorbed doses, especially for non-source organs with substantial mass fraction of blood (lungs, small intestine, colon, oesophagus in case of ^{18}F -FSPG). The considerable influence of the blood even for a radiopharmaceutical with a rapid clearance from the blood, such as ^{18}F -FSPG, suggests that blood should be introduced as a separate compartment in most CPK models and considered as a distinct source region in dosimetric calculations. Hence, blood samples should be included in all PK studies for new tracers if possible.

Disclosure statement

The work was funded by German Federal Ministry of Education and Research, grant 02NUK026. No other potential conflict of interest was reported.

Acknowledgements

We thank Matthias Greiter for fruitful discussions on CPK modelling.

The work was done within the collaborative project PASSOS (<http://passos.helmholtz-muenchen.de>) financed by German Federal Ministry of Education and Research, grant 02NUK026.

References

1. Zanzonico P. Principles of nuclear medicine imaging: planar, SPECT, PET, multi-modality, and autoradiography systems. *Radiat Res.* 2012;177:349-364.
2. Loevinger R, Berman M. MIRDPamphlet no.1 revised: a revised schema for calculating the absorbed dose from biologically distributed radionuclides. The Society of Nuclear Medicine; 1976.
3. Berman M. MIRDPamphlet no. 12: kinetic models for absorbed dose calculations. The Society of Nuclear Medicine; 1977.
4. ICRP, 1988. Radiation dose to patients from radiopharmaceuticals. ICRP Publication 53. *Ann. ICRP* 18.
5. ICRP, 2015. Radiation dose to patients from radiopharmaceuticals: a compendium of current information related to frequently used substances. ICRP Publication 128. *Ann. ICRP* 44.
6. Leggett RW, Williams LR. A proposed blood circulation model for reference man. *Health Phys.* 1995;69:187-201.
7. Guyton AC, Hall JE. Textbook of medical physiology. 11 ed. Philadelphia: Elsevier Saunders; 2006.
8. ICRP, 2002. Basic anatomical and physiological data for use in radiological protection: reference values. ICRP Publication 89. *Ann. ICRP* 32.
9. Sgouros G. Bone marrow dosimetry for radioimmunotherapy: theoretical considerations. *J Nucl Med.* 1993;34:689-694.
10. Bigler RE, Sgouros G. Biological analysis and dosimetry for ¹⁵O-labeled O₂, CO₂, and CO gases administered continuously by inhalation. *J Nucl Med.* 1983;24:431-437.
11. Smolarz K, Krause BJ, Graner FP, et al. (S)-4-(3-¹⁸F-fluoropropyl)-L-glutamic acid: an ¹⁸F-labeled tumor-specific probe for PET/CT imaging-dosimetry. *J Nucl Med.* 2013;54:861-866.
12. ICRP, 1993. Age-dependent doses to members of the public from intake of radionuclides - part 2 ingestion dose coefficients. ICRP Publication 67. *Ann. ICRP* 23.
13. Bellu G, Saccomani MP, Audoly S, D'Angio L. DAISY: a new software tool to test global identifiability of biological and physiological systems. *Comput Methods Programs Biomed.* 2007;88:52-61.

14. Giussani A, Janzen T, Uusijärvi-Lizana H, et al. A compartmental model for biokinetics and dosimetry of ^{18}F -choline in prostate cancer patients. *J Nucl Med.* 2012;53:985-993.
15. Thomas SR, Stabin MG, Chen CT, Samaratunga RC. MIRDPamphlet no. 14 revised: a dynamic urinary bladder model for radiation dose calculations. *J Nucl Med.* 1999;40:102S-123S.
16. Barrett PHR, Bell BM, Cobelli C, et al. SAAM II: simulation, analysis, and modeling software for tracer and pharmacokinetic studies. *Metabolism.* 1998;47:484-492.
17. Bolch WE, Eckerman KF, Sgouros G, Thomas SR. MIRDPamphlet No. 21: a generalized schema for radiopharmaceutical dosimetry-standardization of nomenclature. *J Nucl Med.* 2009;50:477-484.
18. Zankl M, Schlattl H, Petoussi-Hens N, Hoeschen C. Electron specific absorbed fractions for the adult male and female ICRP/ICRU reference computational phantoms. *Phys Med Biol.* 2012;57:4501.
19. ICRP, 2009. Adult reference computational phantoms. ICRP Publication 110. *Ann. ICRP* 39.
20. ICRP, 2008. Nuclear decay data for dosimetric calculations. ICRP Publication 107. *Ann. ICRP* 38.
21. ICRP, 2007. 2007 Recommendations of the International Commission on Radiological Protection. ICRP Publication 103. *Ann. ICRP* 37.
22. Leggett RW, Williams LR. Suggested reference values for regional blood volumes in humans. *Health Phys.* 1991;60:139-154.
23. Smith T, Veall N, Wootton R. Bladder wall dose from administered radiopharmaceuticals: the effects of variations in urine flow rate, voiding interval and initial bladder content. *Radiat Prot Dosim.* 1982;2:183-189.
24. Staaf J, Jacobsson H, Sanchez-Crespo A. A revision of the organ radiation doses from 2-fluoro-2-deoxy-D-glucose with reference to tumour presence. *Radiat Prot Dosimetry.* 2012;151:43-50.
25. Challapalli A, Sharma R, Hallett WA, et al. Biodistribution and radiation dosimetry of deuterium-substituted ^{18}F -fluoromethyl-[1, 2- $^2\text{H}_4$]choline in healthy volunteers. *J Nucl Med.* 2014;55:256-263.

26. Hänscheid H, Fernández M, Eberlein U, Lassmann M. Self-irradiation of the blood from selected nuclides in nuclear medicine. *Phys Med Biol.* 2014;59:1515–1531.
27. Stabin MG, Sparks RB, Crowe E. OLINDA/EXM: the second-generation personal computer software for internal dose assessment in nuclear medicine. *J Nucl Med.* 2005;46:1023-1027.

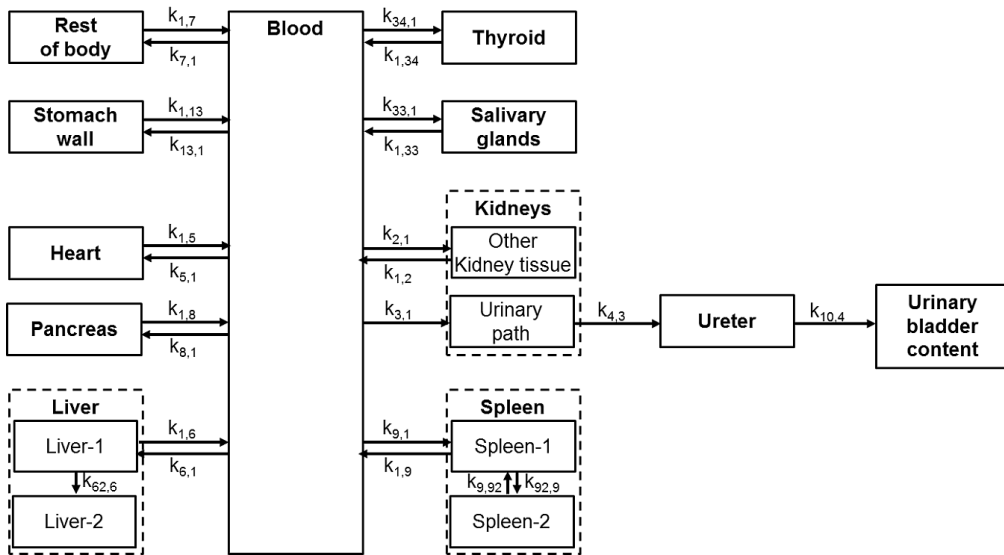


Fig. 1 CPK model structure for ^{18}F -FSPG

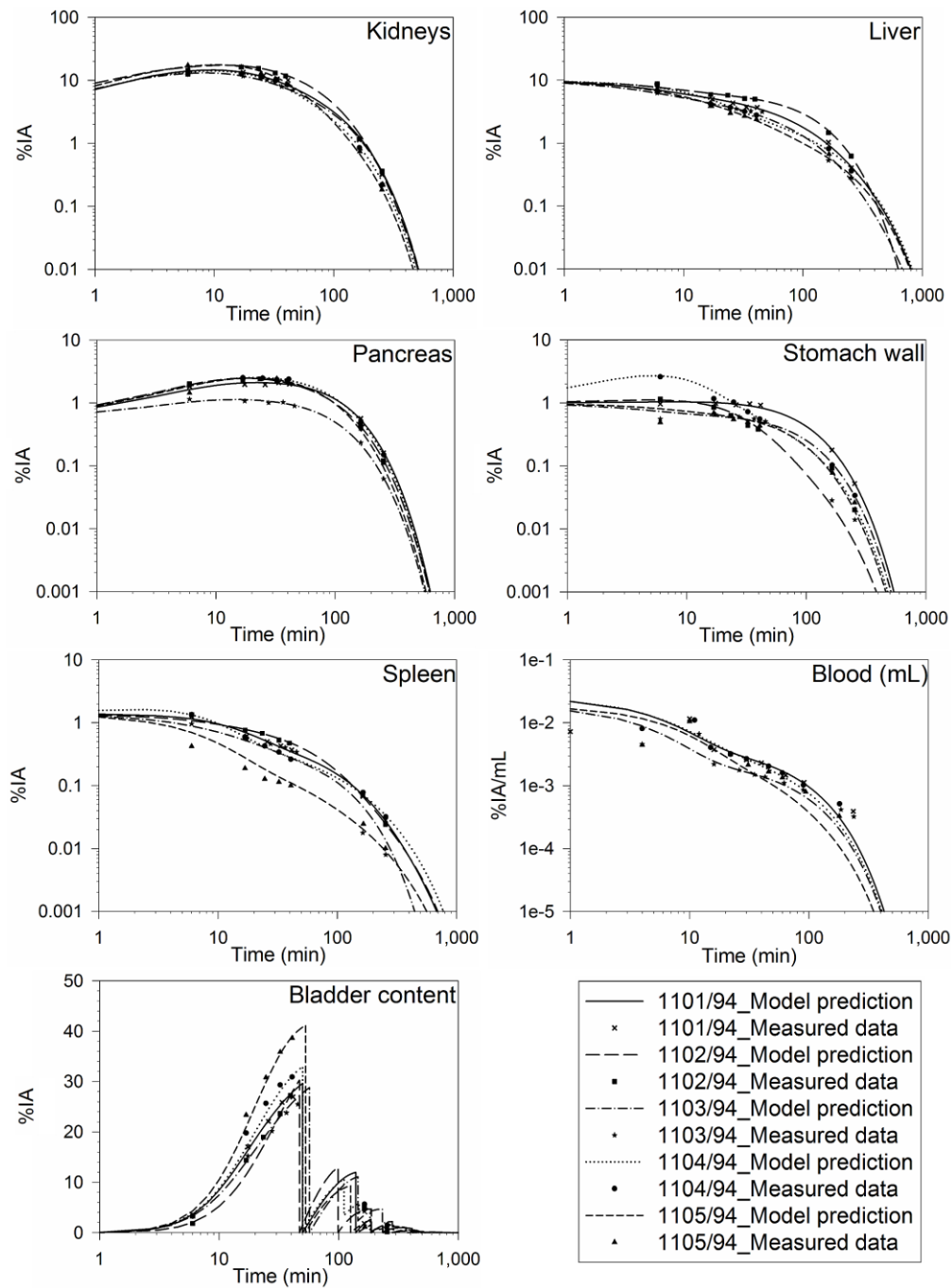


Fig. 2 Resulting CPK model fits for subjects 1101/94–1105/94. The lines are model predictions, discrete points – measured data. For kidneys, liver, pancreas, stomach wall and spleen measured data, obtained from PET images, represent activities of organs along with the activities of blood flowing through them. At $t=0$ (injection time) 100% of IA was in blood. A fraction of blood activity, corresponding to RBV, was attributed to the source organs, resulting in non-zero organ activities at $t=0$. Although such immediate uptake is physiologically not entirely meaningful, we believe this does not have a significant influence on the TIACs due to the fast experimentally observed uptake.

Table 1 Volunteers details and IA of ^{18}F -FSPG [11]

	1101/94- female	1102/94- female	1103/94- male	1104/94- female	1105/94- male
Age, years	58	64	57	63	51
Height, cm	170	170	189	160	168
Weight, kg	90	95	106	65	65
IA, MBq	283	316	275	330	295

Table 2 Organ absorbed-dose coefficients, [mGy/MBq] and effective-dose coefficients, [mSv/MBq]

Target organ	1101/94-female			1102/94-female			1103/94-male			1104/94-female			1105/94-male		
	Concept-1	Concept-2	%Diff	Concept-1	Concept-2	%Diff	Concept-1	Concept-2	%Diff	Concept-1	Concept-2	%Diff	Concept-1	Concept-2	%Diff
Red marrow	8.74E-03	8.28E-03	5.6%	8.12E-03	7.87E-03	3.1%	8.19E-03	7.82E-03	4.7%	8.35E-03	7.93E-03	5.3%	6.76E-03	6.31E-03	7.1%
Colon	1.28E-02	1.07E-02	20.4%	1.09E-02	9.77E-03	11.8%	1.10E-02	9.38E-03	17.1%	1.24E-02	1.04E-02	18.9%	1.01E-02	8.11E-03	24.0%
Lungs	1.12E-02	6.37E-03	76.2%	8.84E-03	6.26E-03	41.3%	8.77E-03	5.88E-03	49.2%	1.03E-02	5.84E-03	75.7%	7.82E-03	4.33E-03	80.8%
Stomach wall	2.92E-02	2.89E-02	1.0%	1.91E-02	1.89E-02	0.6%	1.71E-02	1.70E-02	1.1%	2.57E-02	2.55E-02	1.1%	1.57E-02	1.54E-02	1.9%
Bladder wall	6.33E-02	6.34E-02	-0.1%	5.26E-02	5.27E-02	-0.1%	6.90E-02	6.92E-02	-0.2%	6.40E-02	6.41E-02	-0.1%	6.44E-02	6.46E-02	-0.3%
Oesophagus	1.02E-02	7.20E-03	42.2%	8.63E-03	7.01E-03	23.1%	8.69E-03	6.76E-03	28.7%	9.23E-03	6.46E-03	42.9%	7.29E-03	4.95E-03	47.3%
Liver	2.20E-02	2.09E-02	5.2%	2.74E-02	2.68E-02	2.2%	1.44E-02	1.37E-02	5.3%	1.91E-02	1.81E-02	5.4%	1.38E-02	1.29E-02	6.7%
Thyroid	1.97E-02	1.90E-02	3.5%	1.24E-02	1.20E-02	2.9%	1.35E-02	1.31E-02	3.0%	1.53E-02	1.47E-02	4.1%	9.60E-03	9.12E-03	5.2%
Salivary glands	8.25E-03	7.98E-03	3.3%	5.92E-03	5.77E-03	2.4%	6.52E-03	6.39E-03	1.9%	6.64E-03	6.40E-03	3.7%	4.94E-03	4.79E-03	3.1%
Heart wall	1.42E-02	1.26E-02	12.9%	1.75E-02	1.66E-02	5.3%	1.51E-02	1.41E-02	6.8%	8.11E-03	6.63E-03	22.3%	7.96E-03	6.83E-03	16.6%
Kidneys	1.17E-01	1.16E-01	0.8%	1.48E-01	1.48E-01	0.3%	9.29E-02	9.23E-02	0.7%	9.99E-02	9.91E-02	0.8%	9.78E-02	9.71E-02	0.8%
Adrenals	2.07E-02	1.87E-02	10.6%	2.28E-02	2.18E-02	4.8%	1.84E-02	1.71E-02	7.5%	1.86E-02	1.68E-02	10.7%	1.81E-02	1.66E-02	9.4%
Pancreas	7.45E-02	7.34E-02	1.4%	7.24E-02	7.18E-02	0.7%	3.36E-02	3.28E-02	2.3%	7.74E-02	7.65E-02	1.2%	5.84E-02	5.74E-02	1.6%
Small intestine	1.67E-02	1.43E-02	16.9%	1.48E-02	1.35E-02	9.5%	1.25E-02	1.08E-02	15.1%	1.61E-02	1.39E-02	15.7%	1.15E-02	9.55E-03	20.8%
Spleen	2.17E-02	2.06E-02	5.8%	2.31E-02	2.25E-02	2.8%	1.48E-02	1.39E-02	6.5%	2.04E-02	1.93E-02	5.6%	1.08E-02	9.70E-03	11.1%
Thymus	7.42E-03	5.42E-03	36.9%	6.11E-03	5.05E-03	21.1%	6.20E-03	5.03E-03	23.2%	6.80E-03	4.98E-03	36.6%	4.87E-03	3.45E-03	40.9%
Effective dose coefficient	1.75E-02	1.61E-02	8.5%	1.51E-02	1.43E-02	5.0%	1.32E-02	1.24E-02	6.8%	1.63E-02	1.50E-02	8.3%	1.20E-02	1.10E-02	9.3%

Concept-1: activities in source organs parenchyma, blood is a distinct source

Concept-2: aggregate activities in perfused source organs, without blood as a source

Differences expressed in percentages of concept-2, since this is the "conventional" one